MSc Project

By Freek de Haas; s2783819

Supervised by: Prof. G.S. (Sander) van Doorn

Modelling Sensory Adaptation of Chemotaxis in *Bacillus subtilis*

Modelling Sensory Adaptation of Chemotaxis in *Bacillus subtilis*

Freek J.H. de Haas

Abstract

Exact sensory adaptation, the return of membrane receptors to pre-stimulus activity, is crucial to perform chemotaxis over a wider range of ligand concentrations. Three sensory adaptation systems were identified in *Bacillus subtilis*, two of which are at the focus of this study: (1) the methylation system affects receptor activity by adding and removing methyl groups and (2) the CheC-CheD-CheYp system by regulating CheD binding to the receptor. However their mechanisms are unclear. In this study we modeled three hypothetical mechanisms and analyzed their contribution to sensory adaptation. We showed that shuttling dynamics between site Glu630 and Glu637 of the McpB receptor can result in exact sensory adaptation, only if methylation rates are activity- and site-dependent. We also tested two mechanisms to dissociate CheD from the receptor, (1) either through its interactions with a methylation site or (2) through an increase in affinity for the alternative binding site CheC. Interestingly, both hypotheses suggest that the role of CheD as a receptor activator is negligible.

Introduction

Chemotaxis is the process by which flagellated bacteria sense chemical gradients to bias their movement in more favorable directions [1]. Although their small size is not compatible with spatial sensing to identify these gradients, they have adopted a technique to sense temporal changes through sensory adaptation [5] [17]. In the framework of chemotaxis, exact sensory adaptation describes the return of chemoreceptors to their pre-stimulus activity levels after consistent exposure to an environmental signal. This allows bacteria to respond independently to the absolute level of extracellular ligand concentration.

In a gradient free environment, flagellated bacteria (e.g. *Escherichia coli* and *Bacillus subtilis*) move in a manner akin to a random walk, alternating between straight runs and reorienting tumbles. The multiple flagella complexes located at the cell pole move bacteria forward by rotating counterclockwise (CCW), or make them tumble if one or more flagella switches to a clockwise (CW) rotation. A change in environmental signal temporarily biases the run-tumble frequency depending on the nature of the ligand: attractant or repellent [3]. This deviation from the baseline switching frequency is transitory as the receptors eventually adapt to the new ligand concentration. Ultimately, these repeated temporary biases result in a net movement of the bacteria up a gradient of attractant or down a gradient of repellent, similar to a biased random walk.

Cross-species comparisons of chemotaxis networks have revealed a high degree of homology in its core proteins (CheA, -B, -R, -W and -Y) [12]. Out of 512 analyzed genomes, 206 had at least one homologue of each five core chemotaxis proteins. Despite the homology in chemotaxis proteins, the mechanistic pathways are often different. For example, although *B. subtilis* shares all orthologous chemotaxis proteins with *E.coli* (the model organism to study chemotaxis), a deletion of the CheY response regulator causes *E. coli* to run exclusively and *B. subtilis* to tumble exclusively. Additionally, *B. subtilis* has three extra proteins involved in sensory adaptation (CheV, CheC and CheD) [14] [19]. Studying these molecular networks will allow us to understand how evolution has shaped chemotaxis network structures and how divergent evolution of *B. subtilis* and *E.coli* explains their similarity and differences in their chemotaxis networks.

The signal transduction pathway of *B. subtilis* is well understood. *B. subtilis* senses environmental signals through chemoreceptors, located at distinct locations in the membrane (e.g. McpB and McpC) or in the cytoplasm (e.g. HemAt) [13]. Together, McpB and McpC mediate nearly all taxis to amino acids and carbohydrates and therefore are the best-studied receptor types of *B. subtilis* [13]. Similar to *E. coli*, these membrane receptors form ternary complexes with the adapter protein CheW and histidine autokinase CheA [9] [23]. A change in environmental signal alters the kinase rate and subsequently triggers a phosphorylation cascade response (CheYp, CheVp, CheBp) [8]. CheYp, one of the response regulators, increases the likelihood of the flagella to switch from the basal CW/tumble state to the CCW/run state, by binding to the flagella proteins (FliY) [4]. The concentration of CheYp returns to pre-stimulus levels through sensory adaptation and autodephosphorylation of CheYp.

Three sensory adaptation systems were identified in *Bacillus subtilis*: (1) the methylation system, (2) the CheC-CheD-CheYp system and (3) the CheV system [Figure 1] [20]. The methylation system, which is also present in *E. coli*, adds and removes methyl groups from the receptors using CheR, a methyltransferase, and phosphorylated CheB (CheBp), a methylesterase. The membrane receptors of *B. subtilis* carry glutamine residues which can be methylated to affect the activity of the receptor [10]. CheD, the cornerstone of the CheC-CheD-CheYp system, was shown to activate receptors by binding to the McpB receptor, among others [11]. CheC offers an alternative binding site for CheD and is able to bind CheY/CheYp, resulting in its elaborate network scheme [Figure 1] [19]. CheV is functionally redundant to CheW and is believed to exert its adaptation effect by inhibiting the coupling of receptors with autokinase CheA, depending on its phosphorylated state [2].

Integrating the three sensory adaptation systems of *B. subtilis* in a coherent model is challenging, mainly because the system mechanisms are unclear. First, contrary to *E.*

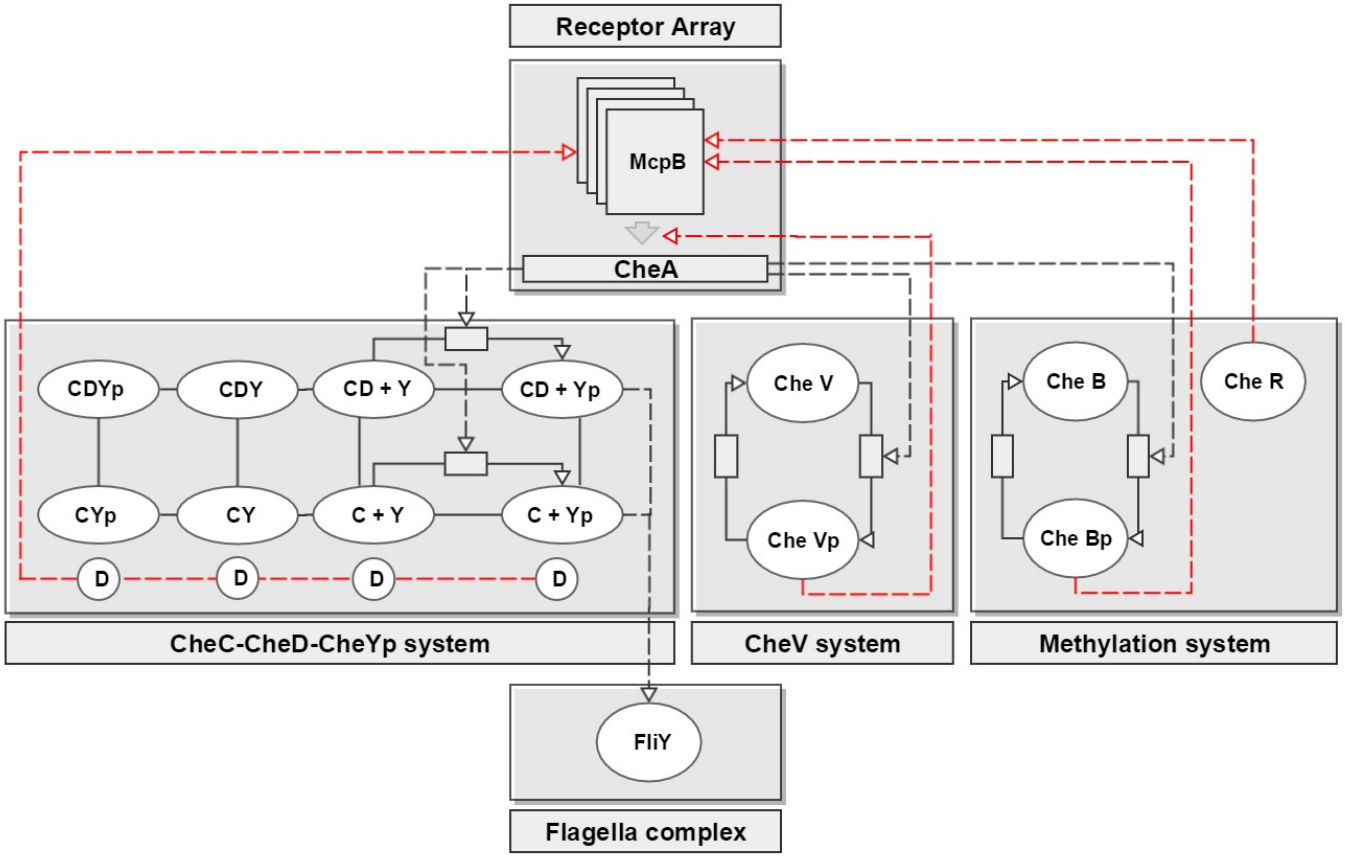

Figure 1: Chemotaxis network of *B. subtilis*. The McpB membrane receptors change the autophosphorylation rate of the kinase (cheA) depending on their activity. CheAp transfers its phosphate group to CheY, CheV and CheB, of which CheY eventually binds to the flagella protein FliY to induce longer runs. The receptor activity is returned to pre-stimulus activity level through three adaptation loops (indicated in red dotted lines). The methylation system adds and removes methyl groups from the receptor through CheB (demethylesterase) and CheR (methyltransferase). The CheV system modifies the binding between the receptor and the autokinase CheA. The CheC-CheD-CheYp system excerts its effect through the regulation of CheD binding to the receptor; CheD being a receptor activator. CheC offers an alternative binding site for CheD and can also bind CheY/CheYp, resulting in the reaction network scheme.

coli, the methylation sites of the receptors have non-additive effects on the receptor activity [28] [10] [26]. Secondly, the empirical data of the methylation sites effects on the receptor activity is still controversial (see [10] [28]). Thirdly, the apparent multiple roles of CheD as an enzyme and reactant in the adaptation process are unclear [11]. Finally, evidence suggests that the multiple adaptation systems increase complexity by adding many higher order interactions to the system [26].

In an attempt to disentangle the mechanisms behind the sensory adaptation systems of *B. subtilis*, we modeled and analyzed three hypotheses of the adaptation mechanisms: one regarding the methylation system (Shuttling hypothesis) and two regarding the CheC-CheD-CheYp system (the Pull- and the Push hypotheses). We simulate the adaptation network using ordinary differential equations (ODE) based on mass action kinetics including a thermodynamics aspect. We explored the parameter space in order to simulate dynamics that resemble predictions based on the three hypotheses.

Materials and Methods

Mathematical Model

To simulate the sensory adaptation of *B. subtilis*, we built a mechanistic model including interactions at the molecular level. The model consists of chemical reactions and receptor state transitions which are simulated according to mass action kinetics including a thermodynamic aspect.

The sensory apparatus in our model is based on the McpB receptor which presents two main advantages: (1) it is the sole receptor involved in asparagine chemotaxis and (2) the experimental data on its methylation effects is the most abundant [10] [28]. Consequently, we use asparagine as the environmental attractant to induce a sensory adaptation response. The receptor (R) has six binary states which are denoted by a sextuple $\Psi = (i, j, k, d, a, l)$. Each of the elements can take value 1 or 0. The activity (a) of the McpB receptor was modeled in two states: active or inactive; where only the active state is capable of activating the kinase. Additionally, the receptor contains three methylation sites (i,j,k), which can be methylated or not, a CheD binding domain (d), to which a CheD can be bound or not, and a ligand binding domain (l), to which a ligand may be bound or not. The resulting 2^6 receptor configurations are modeled, including reactants involved in the phosphorylation cascade, the methylation system and the CheC-CheD-CheYp system [Table 1]

We created reactions for every state transition, including the transitions in methylation states that can occur in the presence of CheBp or CheR, which adds up to 372 reactions. We also included the chemical reactions which are involved in the phosphorylation cascade, the methylation- and the CheC-CheD-CheYp system [Table 2]. CheC has a binding site for CheD and CheY/CheYp, which results in

Table 1: List of reactants and their relative abundance to CheA in the model

Type	Reactants		Ratio [M]
Receptor	R_{ijkdal} [a]		23.0
Phosphorylation cascade	$CheA$	$CheAp$	1.0
	$CheB$	$CheBp$	1.6
	$CheY$	$CheYp$	5.5
CheC/CheD	$CheC$		0.6
	$CheD$		0.9
	CD		
	CDY	$CDYp$	
	CY	CYp	
Other	$CheR$		0.8
	Ligand		0.0 [b]

[a] The receptor is denoted by R, and can be in state i, j, k (methylation sites) , d (CheD bound) , a (Active) and l (Ligand bound) .

[b] step up-stimulus increases ligand concentration to 10.0 and step-down returns it to 0.0

the reaction scheme shown in Figure 1. As a result, CheD can be either bound to the receptor, involved in a complex with CheC, or freely available in the cytoplasm.

Each reaction has a forward (k_{on}) and a backward (k_{off}) rate constant

$$[\text{Substrates}] \underset{k_{off}}{\overset{k_{on}}{\rightleftharpoons}} [\text{Products}]$$

which depend on a kinetic- ($\bar{\text{k}}$) and free energy difference (ΔG) parameter. The free energy difference shifts the ratio of k_{on} (substrate to product) and k_{off} (product to substrate) according to Eq. 1.

$$\frac{k_{on}}{k_{off}} = e^{-\Delta G} \tag{1}$$

To estimate k_{on} and k_{off} separately, we use their geometric mean ($\bar{\text{k}}$).

$$\bar{\text{k}} = \sqrt{k_{on} * k_{off}} \tag{2}$$

Consequently, the forward and backward rates are proportional and inversely proportional to $e^{\Delta G/2}$, respectively [Eq. 3].

$$k_{on} = \bar{\text{k}} e^{\Delta G/2} \quad | \quad k_{off} = \frac{\bar{\text{k}}}{e^{\Delta G/2}} \tag{3}$$

To derive differential equations for the changing reactants over time, we calculate the reaction flux according to mass action kinetics [Eq. 4]

$$\text{flux} = k_{on}[\text{Substrates}] - k_{off}[\text{Products}] \tag{4}$$

The concentration of substrates (S) and products (P) change according to this flux:

$$\frac{d[\text{S}]}{dt} = -\text{flux} \quad \frac{d[\text{P}]}{dt} = +\text{flux} \tag{5}$$

The total flux per reactant is used to calculate the concentrations for the next integration step.

To iterate the differential equations we use the Dormand-Prince Runge-Kutta Integrator (DOPRI), a method for solving ordinary differential equations with an adaptive step size algorithm which uses six function evaluations. They are iterated throughout three consecutive intervals of 200s: the first interval with ligand concentration equal to zero (Ligand = 0), the second interval with Ligand = 10 (step-up stimulus) and the third interval with Ligand = 0 (step-down stimulus). Subsequently, we explored the parameter space and analyzed the resulting dynamics of the three hypothetical adaptation mechanisms to see whether receptor activity returns to pre-stimulus levels after the step-up stimulus at $t = 200$.

Model parameters

The reaction rate constants are calculated based on their kinetic- ($\bar{\text{k}}$) and free energy difference (ΔG) parameters. The free energy difference of the receptor transitions and CheC-CheD-CheYp reactions are built up from additive- and pairwise interaction effects [Table 3]. The free energy difference (ΔG) of a receptor transition for state x in an arbitrary background state (Ψ), is calculated as the sum of its additive effect and pairwise interactions with other states

$$\Delta G_{\Psi \setminus x} = E_x^0 + \sum_{y \epsilon \Psi \setminus x} y E_x^y \tag{6}$$

resulting in a network of energy coupled receptor states [Figure 2]. For reactions involved in the CheC-CheD-CheYp network, the free energy differences depends on six additive energy parameters [Figure 3]. The dephosphorylation cascade reactions depend on the energy of an ATP molecule, which is approximately $E_{ATP} \approx -10.0$ [24] [Figure 4].

The kinetic parameters ($\bar{\text{k}}$) are specific to the chemical reaction or depend on the focal state for the receptor transitions [Table 4]. Furthermore, the reactants and their relative concentrations to CheA (data from [7]) are listed in Table 1.

Signal transduction

Prior to testing the sensory adaptation hypotheses, we specify the parameters for signal transduction: from the extracellular ligand concentration to the intracellular response regulators (CheYp, CheBp). According to mass action kinetics, the equilibrium of the receptor ligand-bound state shifts proportionally to the ligand concentration. Pairwise interaction parameters between receptor states shift the equilibrium of one state depending on the presence of the other. Therefore, further signal transduction is achieved by specifying the energetic coupling between the active and ligand-bound states of the receptor (E_A^L). A positive energy coupling results in a repellent interaction (e.g. a shift in the equilibrium towards inactive state when ligand is bound), whereas a negative coupling results in an attractive interaction (e.g. a shift towards active state when ligand is bound). When the energy coupling equals to zero, the states behave independently from each other. Contrary to *E. coli*, *B. subtilis* increases receptor activity when presented with an attractant stimulus, which indicates a negative energy coupling between the ligand bound- and active state. The additive effects of ligand (E_L^0) and activity (E_A^0) shift the equilibrium of each state irrespective of the receptor background state: a positive value towards the active or ligand-bound state and a negative value towards the inactive or ligand-unbound state respectively.

The energy- and kinetic parameters in Table 3-F6 and Table 4-F6 result in signal transduction. In response to the step-up stimulus at $t = 200$, the receptors transit towards

Table 2: List of reactions included the model.

Reactions			Description
$R_{.....1}$	$\leftrightarrow$	$R_{.....0} + \text{Ligand}$	Transition of receptor ligand state
$R_{....1.}$	$\leftrightarrow$	$R_{....0.}$	Transition of receptor activity state
$R_{...1..}$	$\leftrightarrow$	$R_{...0..} + CheD$	Transition of receptor CheD state
$R_{..1...} + CheR$	$\leftrightarrow$	$R_{..0...} + CheR$	Transition of receptor methylation site 371 with CheR
$R_{..1...} + CheBp$	$\leftrightarrow$	$R_{..0...} + CheBp$	Transition of receptor methylation site 371 with CheBp
$R_{.1....} + CheR$	$\leftrightarrow$	$R_{.0....} + CheR$	Transition of receptor methylation site 630 with CheR
$R_{.1....} + CheBp$	$\leftrightarrow$	$R_{.0....} + CheBp$	Transition of receptor methylation site 630 with CheBp
$R_{1.....} + CheR$	$\leftrightarrow$	$R_{0.....} + CheR$	Transition of receptor methylation site 637 with CheR
$R_{1.....} + CheBp$	$\leftrightarrow$	$R_{0.....} + CheBp$	Transition of receptor methylation site 637 with CheBp
$R_{....1.} + CheA$	$\leftrightarrow$	$R_{....1.} + CheAp$	Phosphorylation of CheA by active receptors
$CheAp + CheB$	$\leftrightarrow$	$CheA + CheBp$	Phosphorylation of methylesterase CheB
$CheBp$	$\leftrightarrow$	$CheB$	Autophosphorylation of CheB
$CheAp + CheY$	$\leftrightarrow$	$CheA + CheYp$	Phosphorylation of response regulator CheY
$CheYp$	$\leftrightarrow$	$CheY$	Autophosphorylation of CheY
$CheC + CheY$	$\leftrightarrow$	$CheCY$	Formation of complex CheCY
$CheCD + CheY$	$\leftrightarrow$	$CheCDY$	Formation of complex CheCDY
$CheC + CheD$	$\leftrightarrow$	$CheCD$	Formation of complex CheCD
$CheCY + CheD$	$\leftrightarrow$	$CheCDY$	Formation of complex CheCDY
$CheC + CheYp$	$\leftrightarrow$	$CheCYp$	Formation of complex CheCYp
$CheCD + CheYp$	$\leftrightarrow$	$CheCDYp$	Formation of complex CheCDYp
$CheCYp + CheD$	$\leftrightarrow$	$CheCDYp$	Formation of complex CheCDYp
$CheCYp$	$\leftrightarrow$	$CheCY$	Dephosphorylation of CheCYp
$CheCDYp$	$\leftrightarrow$	$CheCDY$	Dephosphorylation of CheCDYp

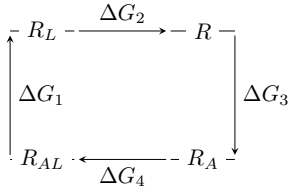

Figure 2: Ligand and Active receptor state energy scheme in background i,j,k,d. R_{AL} (R_{ijkd11}), R_A (R_{ijkd10}), R_L (R_{ijkd01}) and R (R_{ijkd00}). All reactions are reversible, but directionality of arrows indicate in which direction energy differences are calculated. Notice that the sum of the free energy parameters ($\Delta G_1 + \Delta G_2 + \Delta G_3 + \Delta G_4$) adds up to 0, in accordance with the energy conservation principle [Eq. 4].

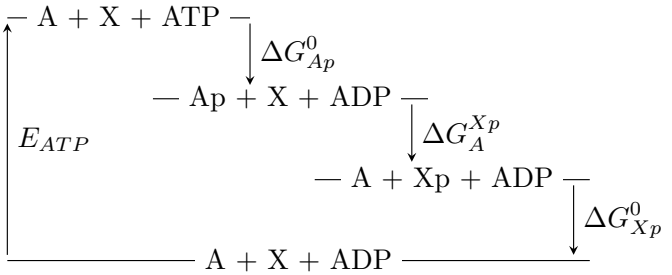

Figure 4: CheA-CheX energy scheme. 'X' represents either 'B' or 'Y'. According to the energy conservation principle, $\Delta G_{Ap} + \Delta G_{A-Xp} + \Delta G_{Xp} + E_{ATP} \approx 0$.

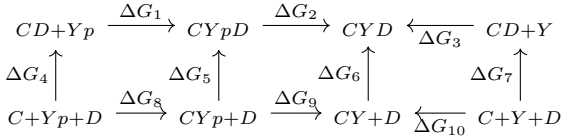

Figure 3: CheC-CheD-CheYp energy scheme. The figure is connected on the left and right side by the phosphorylation reaction of CheY. The free energy differences are based on six additive energy parameters: E^0_{CYp} E^0_{CDYp} E^0_{Yp} E^0_{CY} E^0_{CDY} and E^0_{CD}. Based on these parameters, the free energy differences calculated as follows: $\Delta G_1 = E^0_{CYp} + E^0_{CDYp}$, $\Delta G_2 = E^0_{Yp} + E^0_{CY} - E^0_{CYp} + E^0_{CDY} - E^0_{CDYp}$, $\Delta G_3 = E^0_{CY} + E^0_{CDY}$, $\Delta G_4 = E^0_{CD}$, $\Delta G_5 = E^0_{CD} + E^0_{CDYp}$, $\Delta G_6 = E^0_{CD} + E^0_{CDY}$, $\Delta G_7 = E^0_{CD}$, $\Delta G_8 = E^0_{CYp}$, $\Delta G_9 = E^0_{Yp} + E^0_{CY} - E^0_{CYp}$, $\Delta G_{10} = E^0_{CY}$

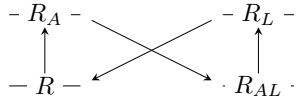

Figure 5: Free energy difference (ΔG) scheme of ligand and active states of the receptor with parameters: $E^0_A = 1$, $E^0_L = 1$, $E^L_A = -2$. The height in this figure represents free energy gaps. Unbound ligand receptors are biased towards the inactive state (position of R_A relative to R) whereas ligand bound receptors are biased towards the active state (position of R_{AL} relative to R_L).

Table 3: List of energy parameters for figure 6,7,8 and 10

Parameter	F6	F7	F8	F10
E_A^0	**1.0**	**3.0**	**1.0**	**1.0**
E_L^0	**1.0**	**-2.0**	**-1.0**	**-2.0**
E_D^0	0.0	0.0	0.0	**4.0**
E_{M371}^0	0.0	0.0	0.0	**4.0**
E_{M630}^0	0.0	**2.0**	0.0	0.0
E_{M637}^0	0.0	**2.0**	0.0	0.0
E_A^L	**-2.0**	**-2.0**	**-2.0**	**-4.0**
E_A^D	0.0	0.0	0.0	**-1.0**
E_A^{M371}	0.0	0.0	0.0	**0.0**
E_A^{M630}	0.0	**-2.5** [a]	0.0	0.0
E_A^{M637}	0.0	**2.0** [b]	0.0	0.0
E_L^D	0.0	0.0	0.0	0.0
E_L^{M371}	0.0	0.0	0.0	0.0
E_L^{M630}	0.0	0.0	0.0	0.0
E_L^{M637}	0.0	0.0	0.0	0.0
E_D^{M371}	0.0	0.0	0.0	**-7.0** [c]
E_D^{M630}	0.0	0.0	0.0	0.0
E_D^{M637}	0.0	0.0	0.0	0.0
E_{M371}^{M630}	0.0	0.0	0.0	0.0
E_{M371}^{M637}	0.0	0.0	0.0	0.0
E_{M630}^{M637}	0.0	**8.0** [d]	0.0	0.0
E_{CD}^0	0.0	0.0	**1.0** [e]	0.0
E_{CY}^0	0.0	0.0	**1.0**	0.0
$E_{CY_p}^0$	0.0	0.0	**1.0**	0.0
E_{CDY}^0	0.0	0.0	**2.0**	0.0
$E_{CDY_p}^0$	0.0	0.0	**-1.0**	0.0
$\Delta G_{R_{ijkdil}}^{Ap}$	**-3.0**	**-3.0**	**-3.0**	**-3.0**
ΔG_A^{Bp}	**-1.0**	**-1.0**	0.0	**-1.0**
ΔG_A^{Yp}	**-1.0**	**-1.0**	**-1.0**	**-1.0**
ΔG_{Bp}^0	**-3.0**	**-3.0**	0.0	**-3.0**
ΔG_{Yp}^0	**-3.0**	**-3.0**	**-5.0**	**-3.0**

[a] Methylation site 630 activates the receptor

[b] Methylation site 637 deactivates the receptor

[c] The strong negative energy coupling dissociates CheD from the receptor when site 371 is removed.

[d] The strong positive energy coupling between methylation site 630 and 637 causes a repellent interaction which favors shuttling dynamics.

[e] Derived from Yuan et al (2012)

the ligand-bound and active state, followed by a step-down stimulus at $t = 400$ which returns the dynamics to pre-stimulus levels [Figure 6]. The free energy differences for the active and ligand bound transitions are shown in Figure 5. The response regulators CheYp and CheBp change proportionally to the level of active receptors. Notice that the free energy parameters are consistent with $E_{ATP} \approx -10.0$.

Results

Three mechanistic hypotheses for sensory adaptation were tested: one involved in the methylation system (Shuttling hypothesis) and two involved in the CheC-CheD-CheYp system (the Pull- and the Push hypotheses).

Methylation System

Background. Both CheR (the methyltransferase) and phosphorylated CheB (the methylesterase), are present in *B. subtilis* and *E. coli*. However, the methylation sites of the *B. subtilis* receptors, unlike those of *E. coli*, have site-specific effects on the receptor activity. As shown by Kirby et al (1999), the sensory adaptation in *B. subtilis* is accompanied by rapid demethylation (1-2 minutes), both with the addition and removal of attractant [15]. The methylation sites of the McpB receptor are closely spaced at sites Gln371, Glu630 and Glu637 (hereafter named 'site 371', 'site 630' and 'site 637'). Results from Zimmer et al (2000) suggest that methylation at site 630 increases receptor activity, at site 637 decreases it and at site 371 seems to have no direct effect.

Parameters. According to the results from Zimmer et al (2000), a simple model was proposed in which the shuttling of methyl groups between site 630 and 637 is responsible for adaptation (shuttling hypothesis). In order to test this hypothesis, we chose parameters that induce shuttling dynamics between site 630 and site 637. Based on the results from Zimmer et al (2000), the energy coupling between site 630 and activity was set to $E_A^{M630} = -3.0$ (shifting equilibrium towards active state when methylated at site 630), whereas between site 637 and activity, it was set to $E_A^{M637} = 3.0$ (shifting equilibrium towards inactive state when methylated at site 637). The remaining energy- and kinetic parameters are shown in Table 3-F7 and Table 4-F7, respectively.

Results. With the chosen parameters we were able to simulate shuttling dynamics between sites 630 and 637. However, to obtain sensory adaptation it was necessary to include activity- and/or site-dependent methylation rates. We assumed demethylation at site 637 when the receptor is inactive, and methylation when active. Conversely, at site 630, demethylation occurs when the receptor is active and methylation when inactive. Further tuning of the methylation rate parameters resulted in *exact* sensory adaptation [Figure 7].

CheC-CheD-CheYp System

Background. In addition to the core chemotaxis proteins of *E. coli*, *B. subtilis* expresses CheC and CheD as part of the CheC-CheD-CheYp system. The cornerstone of this system is CheD, which was experimentally shown to bind the membrane receptors and increase their activity [11]. CheD is also known to bind CheC. Mutating residues in CheC or CheD that abolish binding to each other have deleterious effects on chemotaxis behavior, which underlines the importance of their interaction [27]. Paradoxically, CheC and CheD also have enzymatic activities: CheC is a CheYp phosphatase and CheD is a deamidase for particular glutamine residues on thee receptors [25] [16]. However, mutated residues that abolish their enzymatic activities have relatively small effects on chemotaxis [27]. Moreover, CheYp increases the affinity of CheC for CheD.

Pull hypothesis

A mechanism was proposed in which CheC regulates the CheD binding to the receptor through a competitive binding mechanism (the pull hypothesis) [20]. When receptor activity increases, more CheC-CheYp complex is formed which

Table 4: Kinetic parameters for figure 6,7,8 and 10

Reactions			**F6**	**F7**	**F8**	**F10**
$R_{.....1}$	$\leftrightarrow$	$R_{.....0}$ ‘	**10.0**	**10.0**	**10.0**	**10.0**
$R_{....1.}$	$\leftrightarrow$	$R_{....0.}$	**100.0**	**100.0**	**100.0**	**100.0**
$R_{...1..}$	$\leftrightarrow$	$R_{...0..} + CheD$	0.0	0.0	**10.0**	**10.0**
$R_{..1.1.} + CheR$	$\leftrightarrow$	$R_{..0.1.} + CheR$	0.0	**4.0**	0.0	0.0
$R_{..1.1.} + CheBp$	$\leftrightarrow$	$R_{..0.1.} + CheBp$	0.0	0.0	0.0	0.0
$R_{..1.0.} + CheR$	$\leftrightarrow$	$R_{..0.0.} + CheR$	0.0	0.0	0.0	0.0
$R_{..1.0.} + CheBp$	$\leftrightarrow$	$R_{..0.0.} + CheBp$	0.0	**2.0**	0.0	0.0
$R_{.1..1.} + CheR$	$\leftrightarrow$	$R_{.0..1.} + CheR$	0.0	0.0	0.0	0.0
$R_{.1..1.} + CheBp$	$\leftrightarrow$	$R_{.0..1.} + CheBp$	0.0	**4.0**	0.0	0.0
$R_{.1..0.} + CheR$	$\leftrightarrow$	$R_{.0..0.} + CheR$	0.0	**0.05**	0.0	0.0
$R_{.1..0.} + CheBp$	$\leftrightarrow$	$R_{.0..0.} + CheBp$	0.0	0.0	0.0	0.0
$R_{1...1.} + CheR$	$\leftrightarrow$	$R_{0...1.} + CheR$	0.0	0.0	0.0	0.0
$R_{1...1.} + CheBp$	$\leftrightarrow$	$R_{0...1.} + CheBp$	0.0	0.0	0.0	**1.0**
$R_{1...0.} + CheR$	$\leftrightarrow$	$R_{0...0.} + CheR$	0.0	0.0	0.0	**0.1**
$R_{1...0.} + CheBp$	$\leftrightarrow$	$R_{0...0.} + CheBp$	0.0	0.0	0.0	0.0
$R_{....1.} + CheA$	$\leftrightarrow$	$R_{....1.} + CheAp$	**10.0**	**10.0**	**10.0**	**10.0**
$CheAp + CheB$	$\leftrightarrow$	$CheA + CheBp$	**20.0**	**20.0**	**20.0**	**20.0**
$CheBp$	$\leftrightarrow$	$CheB$	**15.0**	**15.0**	**15.0**	**15.0**
$CheAp + CheY$	$\leftrightarrow$	$CheA + CheYp$	**80.0**	**80.0**	**80.0**	**80.0**
$CheYp$	$\leftrightarrow$	$CheY$	**0.01**	**0.01**	**0.01**	**0.01**
$CheC + CheY$	$\leftrightarrow$	$CheCY$	0.0	0.0	0.0	0.0
$CheCD + CheY$	$\leftrightarrow$	$CheCDY$	0.0	0.0	**10.0**	0.0
$CheC + CheD$	$\leftrightarrow$	$CheCD$	0.0	0.0	**0.001**	0.0
$CheCY + CheD$	$\leftrightarrow$	$CheCDY$	0.0	0.0	0.0	0.0
$CheC + CheYp$	$\leftrightarrow$	$CheCYp$	0.0	0.0	**10.0**	0.0
$CheCD + CheYp$	$\leftrightarrow$	$CheCDYp$	0.0	0.0	0.0	0.0
$CheCYp + CheD$	$\leftrightarrow$	$CheCDYp$	0.0	0.0	**10.0**	0.0
$CheCYp$	$\leftrightarrow$	$CheCY$	0.0	0.0	0.0	0.0
$CheCDYp$	$\leftrightarrow$	$CheCDY$	0.0	0.0	**10.0**	0.0

Table 5: List of energy parameters and their ΔG and K_D parameters. The K_D parameters are obtained from Yuan et al. 2012. There was normalization for temperature and the Boltsman constant necessary because ΔG in our model includes the temperature and boltsman units.

Energy parameters	K_D	ΔG
E^0_{CD}	3.95 mM	1.37
E^0_{CDY}	7.01 mM	1.95
E^0_{CDYp}	0.546 mM	-0.61

functions as an alternative binding target for CheD, thereby 'pulling' CheD off the receptor.

Parameters. To dissociate $CheD$ from the receptor, we set parameters to increase the likelihood of $CheYp$ dephosphorylation through its interaction with $CheC$ and $CheD$, thereby trapping $CheD$ in the complex CD, rather than through auto-dephosphorylation. The free energy difference parameters for the CheC-CheD binding were estimated from experimental data and converted to free energy coefficients [Table 5]. The remaining parameters were set so $CheYp$ could interact with $CheC$ to form complex CYp from where, through the intermediate states $CYpD$ and CYD, complex $CD+Y$ could be formed [Figure 9]. We set the reaction rates to relatively high rates to allow quick formation of CD, whereas the disintegration of complex CD and the immediate (de)phosphorylation of $CheYp$ were set at a much lower rates [Table 3-F8] [Table 4-F8].

Results. The step-up stimulus at $t = 200$ removed CheD partly from the receptor and returned to pre-stimulus levels after the step-down stimulus at $t = 400$ [Figure 8]. The receptor activity did not show signs of adaptation.

Push hypothesis

An alternative mechanism to dissociate CheD from the receptor is by actively 'pushing' CheD off through the interaction with an alternative receptor state (push hypothesis). This mechanism is considered less probable because CheC mutants who reduce phosphatase activity are able to adapt, which suggests that CheC's main function is to interact with CheD [27]. However, both mechanisms are not mutually exclusive in the modulation of CheYp levels. We explored the possibility for CheD to become dissociated from the receptor through its interaction with an arbitrary methylation site. For these simulations we used site 371.

Parameters. As a response to changes in the ligand concentration, site 371 is able to 'push' CheD off the receptor. Due to the increase in methylesterase ($CheBp$), methylation sites are easily removed. Therefore, the effect of a methyl group dissociation will be relatively stronger than its association. We set the pairwise interaction between $CheD$ and methylation site 371 to $E_D^{M371} = -7.0$ in order to dissociate $CheD$ off the receptor, together with site 371. As CheD is a receptor activator, the energy coupling between activity and $CheD$ was set to $E_A^D = -1.0$. To distinguish the effect of $CheD$ dissociation on sensory adaptation, the energy coupling between activity and site 371 was set to zero ($E_A^{M371} = 0$). The remaining energy- and kinetic parameters are shown in Table 3-F10 and Table 4-F10, respectively.

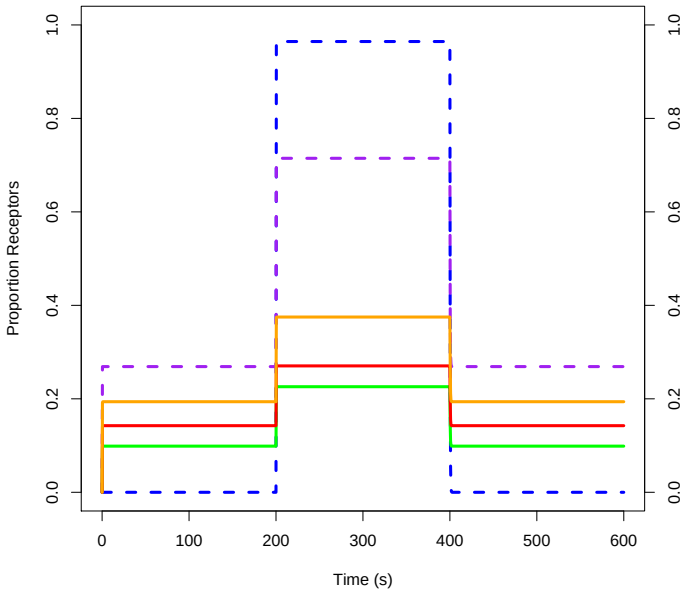

Figure 6: The change in the proportion of ligand (blue dotted) and active (purple dotted) states of the receptor and the subsequent CheAp (green), CheYp (orange) and CheBp (red) response over time. Parameters are shown in Table 3-F6 and Table 4-F6.

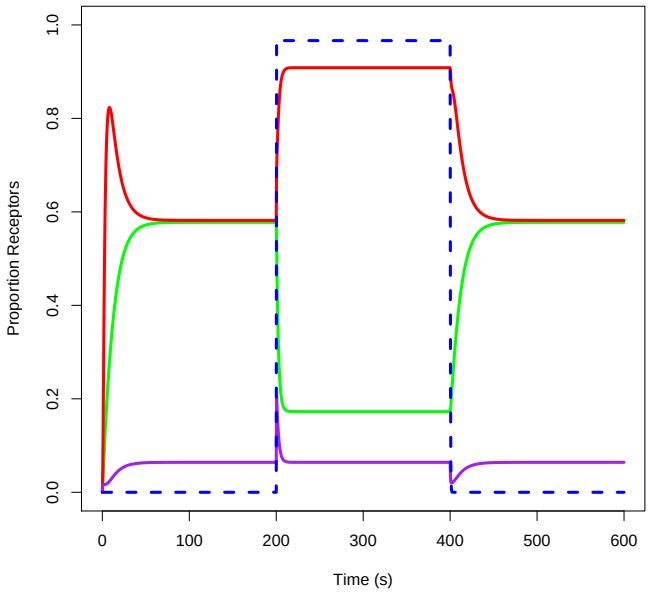

Figure 7: Methylation Shutteling Hypothesis (Zimmer et al.), according to the model parameters in Table 3-F2 and table 4-F2. The proportion of receptors methylated at site 637 (red) and site 630 (green) and the activity (purple) are shown. The blue dotted line represents the proportion of ligand bound receptors over time.

Results. With the chosen parameter set, we were able to show that a large proportion of receptors removed CheD following the step-up stimulus at $t = 200$ [Figure 10a,b]. Because site 371 behaved independently of the activity, receptor adaptation can solely be the result of CheD dissociation. However, we only observed a very small effect on the sensory adaptation.

Discussion

In this study we have explored potential adaptation mechanisms of the methylation and CheC-CheD-CheYp system of *B. subtilis*. We tested the possibility for methyl group shuttling between site 630 and 637 of the McpB receptor (shuttling hypothesis) and we explored two mechanisms to regulate CheD binding to the receptor (pull- and push hypothesis). The methylation results suggest that perfect sensory adaptation is possible under restrictive assumptions on the activity- and site-specific methylation rates. With respect to the CheD regulation, we showed that both the pull- and push hypotheses succeeded in partly dissociating CheD from the receptor. The pull hypothesis temporarily trapped CheD in a complex with CheC, while the push hypothesis dissociated CheD through the energy coupling with an arbitrary methylation site. Although the mechanism of the push hypothesis was more effective to remove CheD from the receptor, both mechanisms had a negligible effect on receptor adaptation.

Sensory Adaptation

Exact sensory adaptation is achieved when, irrespective of the ligand concentration, the receptor activity at equilibrium returns to the same level. The chemotaxis system adapts by adjusting the intracellular receptor states i,j,k and d depending on the ligand concentration, meaning that the steady state levels of methylation- and CheD states vary with ligand concentration in order to maintain the same steady state activity level. However, sensory adaptation requires that CheYp behaves independently of the ligand concentration at steady state (and therefore also CheBp), while also affecting the receptor states i,j,k and d.

Mello Yu et al (2003) built a simplified *E. coli* model to investigate under which conditions CheYp behaves independent of the ligand concentration [18]. One of the conditions was that rates between the methylation states and CheR/CheBp are linearly related to the activity of the receptor. In models of *E. coli* sensory adaptation, it is generally assumed that methylation happens sequentially and that CheB only demethylates active receptors, while CheR methylates inactive receptors. Our results indicate that, similar to *E. coli*, *B. subtilis* requires activity- and site-dependent methylation in order to perfectly adapt. However, empirical evidence is inconclusive on this matter. Our results highlight again the importance of such a mechanism in order to obtain perfect sensory adaptation.

Our results showed that activity and site dependent methylation result in a stable CheYp equilibrium, independent of the ligand concentrations. To obtain exact sensory adaptation for the CheC-CheD-CheYp system, CheYp and CheD return to pre-stimululs concentrations. Therefore, the mechanism of the pull hypothesis is not able to produce exact sensory adaptation. Nevertheless, it is possible for CheD to improve the adaptation response with the help of an additional system, such as the methylation system (push hypothesis).

CheD abundance

Although CheD was dissociated from the receptor successfully, its effect on the sensory adaptation was negligible. This is probably due to its low abundance inside the cell [7]. The ratio of CheD to receptors is approximately 1 : 23,

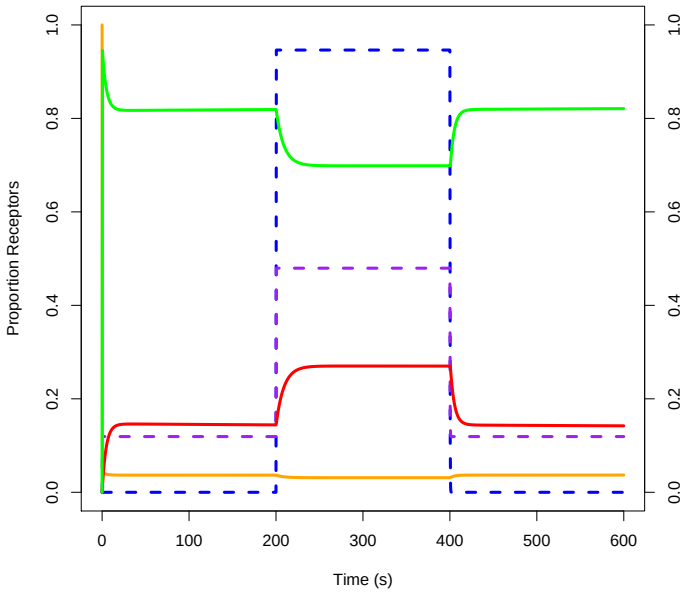

Figure 8: CheD dynamics of the pull hypothesis, showing the abundance of CheD bound to the receptor (green), bound to CheC (red) and unbound (orange). The dotted lines represent the proportion of ligand bound (blue) and active (purple) receptors. Parameters are shown in Table 3-F8 and Table 4-F8.

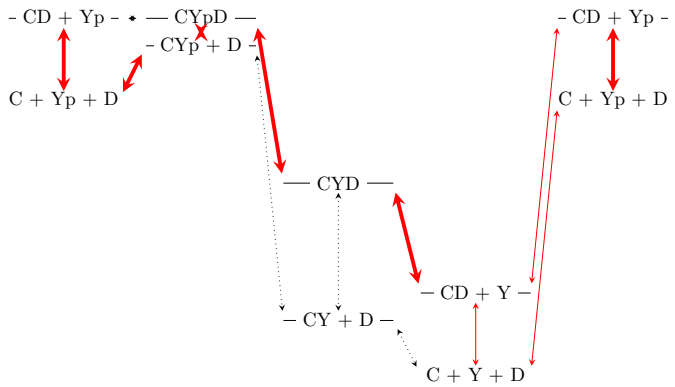

Figure 9: CheC-CheD-CheYp free energy difference (ΔG) scheme. The thickness of the red lines indicate their relative rate constants, whereas the black lines represent a rate constant of zero. Parameters are: $E_{CD} = 1.5$, $E_{CY} = 1$, $E_{CYp} = 1$, $E_{CDY} = 2$, $E_{CDYp} = -1$, $E_{Yp} = -5$.

(a)

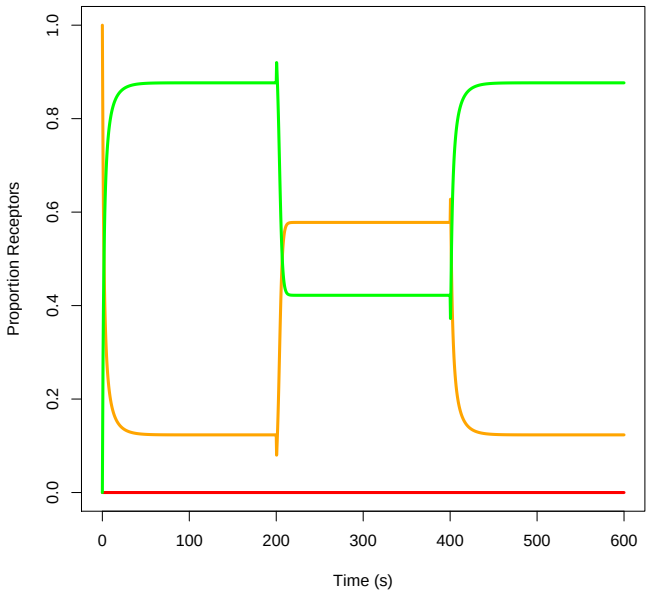

(b)

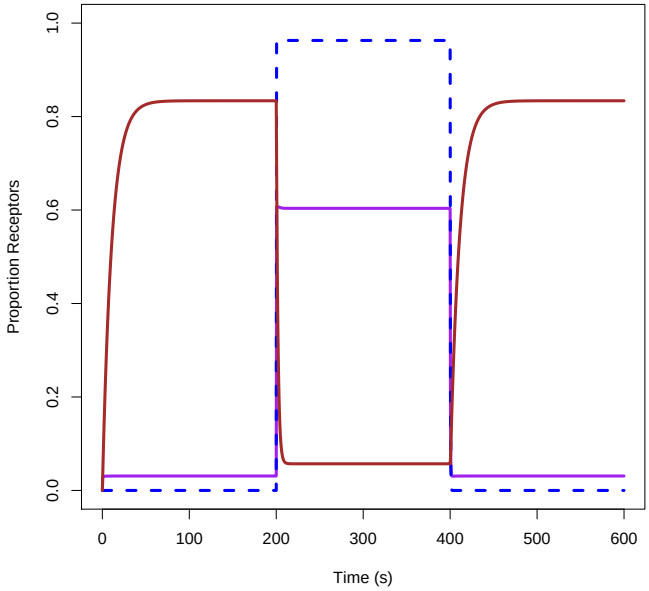

Figure 10: CheD and methylation dynamics of the push hypothesis. (a) shows the proportion of receptors that are bound by CheD (green), in a complex with CheC (red) or unbound (orange). (b) The proportion of receptors methylated at site 371 (brown), active (purple) and ligand bound (dotted blue). The parameters can be found in Table 3-F10 and Table 4-F10.

which implies that CheD has an effective influence of 5 percent on the receptor activity. Even though CheD is thought to play an important role on the adaptation process [27], our results suggest that CheD's functionality as a receptor activator is negligible. We therefore hypothesize that CheD binding does not directly affect the receptor activity, but rather has indirect effects on the methylation system. In the 20 minutes following rapid demethylation, a slow remethylation of the receptors takes place [15]. Mutants in the CheC-CheD-CheYp system were shown to affect the methylation level of the receptors: receptors of CheC-null mutants are methylated at two times wild-type level, receptors of CheD-null mutants are weakly methylated, and receptors of CheY-null mutants do not remethylate after the addition of attractant [21] [22] [15]. After receptor activation and subsequent CheD dissociation from the receptor, CheD's slow return to the receptor shifts the methylation state equilibrium, causing slow remethylation. This hypothetical mechanism depends on the pull-hypothesis to remove CheD from the receptor, which is in line with the findings from Yuan et al (2012) and can explain its role in methylation dynamics.

Site-specific methylation

Zimmer's (2000) results on the effects of specific methylation sites on receptor activity, were recently challenged by a study from Glekas et al (2011) [10]. Using a similar technique, their results showed that sites 630 and 637 reduce receptor (McpB) activity but do not affect the affinity for

asparagine. On the other hand, site 371 increases the receptor's affinity for asparagine and its ability to activate the CheA kinase. They concluded that activity and affinity might be differently regulated. Therefore, the pairwise interaction between each methylation site and the receptor activity needs to be further analyzed.

Adaptive receptor clusters

Chemotaxis systems have the ability to sense and respond to extremely low concentrations of ligands (i.e. 5 nM of asparagine). Additionally, chemotactic behavior is observed in a wide range of concentrations, up to 5 orders of magnitude (i.e. up to 1mM of asparagine). The ability to sense extremely low concentrations is probably the result of receptor clustering in the membrane, which allows neighboring cells to influence each other's activity. This clustering increases the sensitivity to extracellular ligands but severely diminishes the range of concentrations over which the sensory apparatus works (Bray et al, 1998) [6]. However, a combination of low threshold response and wide dynamic range can be attained if the cell has both clusters and single receptors on its surface, especially if the clustering can adapt to external conditions. We propose a mechanisms for CheV to function as a regulator in the receptor clustering. This would mean that the trade-off between amplitude- and range of sensitivity is being optimized by the CheV system.

Conclusions

Our results suggest that, similar to *E. coli*, models for *B. subtilis* require activity- and site-dependent methylation effects to obtain exact sensory adaptation. We also obtained new insights in the CheC-CheD-CheYp system. We showed that CheD's apparent role as a receptor activator is effectively negligible to sensory adaptation. Therefore our results points to a different mechanism for the CheC-CheD-CheYp system.

References

[1] Julius Adler. Chemotaxis in bacteria. *Science*, 153(3737):708–716, 1966.

[2] Roger P Alexander, Andrew C Lowenthal, Rasika M Harshey, and Karen M Ottemann. Chev: Chew-like coupling proteins at the core of the chemotaxis signaling network. *Trends in microbiology*, 18(11):494–503, 2010.

[3] Howard C Berg, Douglas A Brown, et al. Chemotaxis in escherichia coli analysed by three-dimensional tracking. *Nature*, 239(5374):500–504, 1972.

[4] David S Bischoff and George W Ordal. Identification and characterization of fliy, a novel component of the bacillus subtilis flagellar switch complex. *Molecular microbiology*, 6(18):2715–2723, 1992.

[5] Steven M Block, Jeffery E Segall, and Howard C Berg. Adaptation kinetics in bacterial chemotaxis. *Journal of bacteriology*, 154(1):312–323, 1983.

[6] Dennis Bray, Matthew D Levin, and Carl J Morton-Firth. Receptor clustering as a cellular mechanism to control sensitivity. *Nature*, 393(6680):85–88, 1998.

[7] Vincent J Cannistraro, George D Glekas, Christopher V Rao, and George W Ordal. Cellular stoichiometry of the chemotaxis proteins in bacillus subtilis. *Journal of bacteriology*, 193(13):3220–3227, 2011.

[8] Joseph J Falke, Randal B Bass, Scott L Butler, Stephen A Chervitz, and Mark A Danielson. The two-component signaling pathway of bacterial chemotaxis: a molecular view of signal transduction by receptors, kinases, and adaptation enzymes. *Annual review of cell and developmental biology*, 13:457, 1997.

[9] Julie A Gegner, Daniel R Graham, Amy F Roth, and Frederick W Dahlquist. Assembly of an mcp receptor, chew, and kinase chea complex in the bacterial chemotaxis signal transduction pathway. *Cell*, 70(6):975–982, 1992.

[10] George D Glekas, Joseph R Cates, Theodore M Cohen, Christopher V Rao, and George W Ordal. Site-specific methylation in bacillus subtilis chemotaxis: effect of covalent modifications to the chemotaxis receptor mcpb. *Microbiology*, 157(1):56–65, 2011.

[11] George D Glekas, Matthew J Plutz, Hanna E Walukiewicz, George M Allen, Christopher V Rao, and George W Ordal. Elucidation of the multiple roles of ched in bacillus subtilis chemotaxis. *Molecular microbiology*, 86(3):743–756, 2012.

[12] Rebecca Hamer, Pao-Yang Chen, Judith P Armitage, Gesine Reinert, and Charlotte M Deane. Deciphering chemotaxis pathways using cross species comparisons. *BMC systems biology*, 4(1):3, 2010.

[13] David W Hanlon and George W Ordal. Cloning and characterization of genes encoding methyl-accepting chemotaxis proteins in bacillus subtilis. *Journal of Biological Chemistry*, 269(19):14038–14046, 1994.

[14] Ece Karatan, Michael M Saulmon, Michael W Bunn, and George W Ordal. Phosphorylation of the response regulator chev is required for adaptation to attractants during bacillus subtilischemotaxis. *Journal of Biological Chemistry*, 276(47):43618–43626, 2001.

[15] John R Kirby, Michael M Saulmon, Christopher J Kristich, and George W Ordal. Chey-dependent methylation of the asparagine receptor, mcpb, during chemotaxis in bacillus subtilis. *Journal of Biological Chemistry*, 274(16):11092–11100, 1999.

[16] Christopher J Kristich and George W Ordal. Bacillus subtilis ched is a chemoreceptor modification enzyme required for chemotaxis. *Journal of Biological Chemistry*, 277(28):25356–25362, 2002.

[17] Robert M Macnab and DE Koshland. The gradient-sensing mechanism in bacterial chemotaxis. *Proceedings of the National Academy of Sciences*, 69(9):2509–2512, 1972.

[18] Bernardo A Mello and Yuhai Tu. Perfect and near-perfect adaptation in a model of bacterial chemotaxis. *Biophysical journal*, 84(5):2943–2956, 2003.

[19] Travis J Muff and George W Ordal. The chec phosphatase regulates chemotactic adaptation through ched. *Journal of Biological Chemistry*, 282(47):34120–34128, 2007.

[20] Christopher V Rao, George D Glekas, and George W Ordal. The three adaptation systems of bacillus subtilis chemotaxis. *Trends in microbiology*, 16(10):480–487, 2008.

[21] Mia Mae L Rosario, John R Kirby, Daniel A Bochar, and George W Ordal. Chemotactic methylation and behavior in bacillus subtilis: role of two unique proteins, chec and ched. *Biochemistry*, 34(11):3823–3831, 1995.

[22] Mia Mae L Rosario and George W Ordal. Chec and ched interact to regulate methylation of bacillus subtilis methyl-accepting chemotaxis proteins. *Molecular microbiology*, 21(3):511–518, 1996.

[23] MM Rosario, Kurt L Fredrick, George W Ordal, and John D Helmann. Chemotaxis in bacillus subtilis requires either of two functionally redundant chew homologs. *Journal of bacteriology*, 176(9):2736–2739, 1994.

[24] J. Rosing and E.C. Slater. The value of g degrees for the hydrolysis of atp. *Biochim Biophys Acta. 267(2):275-90. Table VIII p. 287*, 1972.

[25] Hendrik Szurmant, Travis J Muff, and George W Ordal. Bacillus subtilis chec and fliy are members of a novel class of cheyp-hydrolyzing proteins in the chemotactic signal transduction cascade. *Journal of Biological Chemistry*, 279(21):21787–21792, 2004.

[26] Hanna E Walukiewicz, Payman Tohidifar, George W Ordal, and Christopher V Rao. Interactions among the three adaptation systems of bacillus subtilis chemotaxis as revealed by an in vitro receptor-kinase assay. *Molecular microbiology*, 93(6):1104–1118, 2014.

[27] Wei Yuan, George D Glekas, George M Allen, Hanna E Walukiewicz, Christopher V Rao, and George W Ordal. The importance of the interaction of ched with chec and the chemoreceptors compared to its enzymatic activity during chemotaxis in bacillus subtilis. 2012.

[28] Michael A Zimmer, Joseph Tiu, Marissa A Collins, and George W Ordal. Selective methylation changes on the bacillus subtilis chemotaxis receptor mcpb promote adaptation. *Journal of Biological Chemistry*, 275(32):24264–24272, 2000.

Supplementary Materials

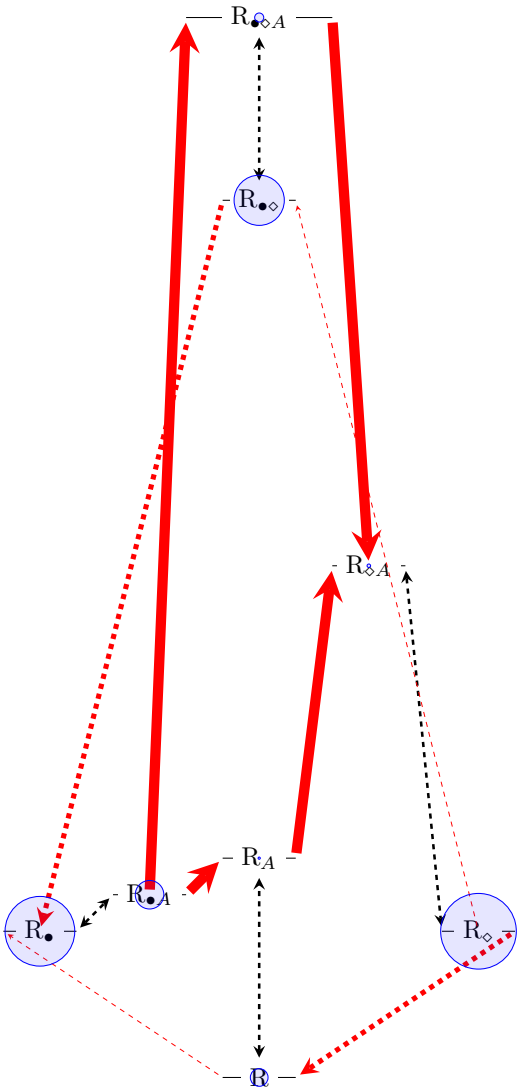

Figure 11: Receptor abundance $t = 200$, shown in an free energy difference scheme of receptor states: Methylation 630 (•), 637 (◇) and Activity (A). The abundance at t = 200 is represented by the surface area of the circles; the thickness of the lines represent the relative reaction rates. Red lines indicate that a reaction can only occur in one direction. The states connected by solid lines are part of the active representation of the receptor, which collectively move depending on the Y_A^L parameter. The parameter are: $E_A^0 = 3$, $E_L^0 = -2$, $E_{M630}^0 = 2$, $E_{M637}^0 = 2$, $E_A^{M630} = -2.5$, $E_A^{M637} = 2$, $E_{M630}^{M637} = 8$. $k_{AM630}^{CheBp} = 4.0$, $k_{M630}^{CheBp} = 0.0$, $k_{AM6307}^{CheBp} = 0.0$, $k_{M637}^{CheBp} = 2.0$, $k_{AM630}^{CheR} = 0.0$, $k_{M630}^{CheR} = 0.05$, $k_{AM6307}^{CheR} = 4.0$, $k_{M637}^{CheR} = 0.0$

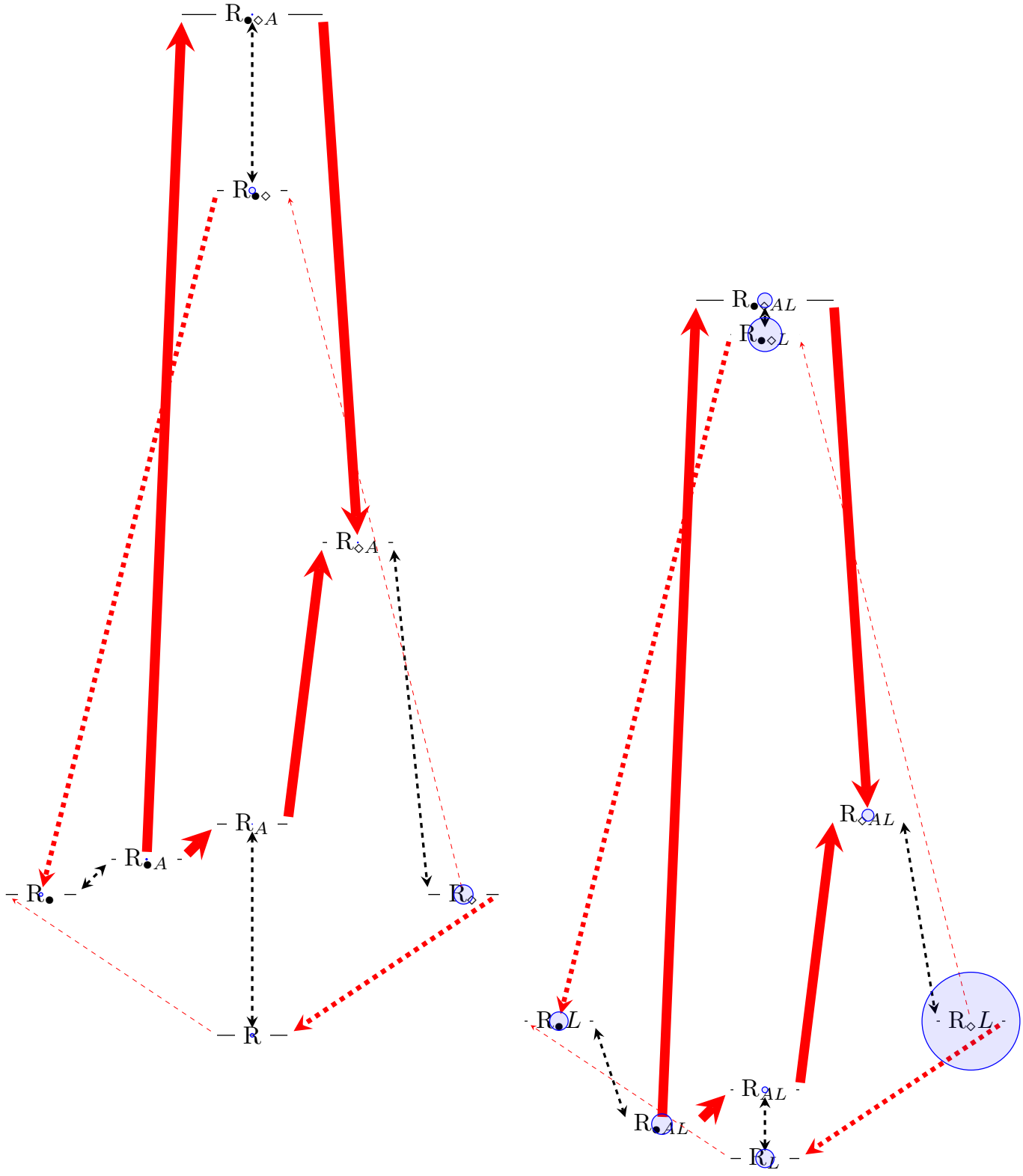

Figure 12: Receptor abundance at 400 time units shown in an energy scheme of Methylation 630, 637 Ligand and Activity. The abundance is represented by the surface area. The receptor is denoted by Y and can be in state: A = Active, $\bullet$ = Site 630, $\diamond$ = Site 637, L = Ligand. The parameter values are: $E_A^0 = 3$, $E_L^0 = -2$, $E_{M630}^0 = 2$, $E_{M637}^0 = 2$, $E_A^{M630} = -2.5$, $E_A^L = -2$, $E_A^{M637} = 2$, $E_L^{M630} = 0$, $E_L^{M637} = 0$, $E_{M630}^{M637} = 8$.

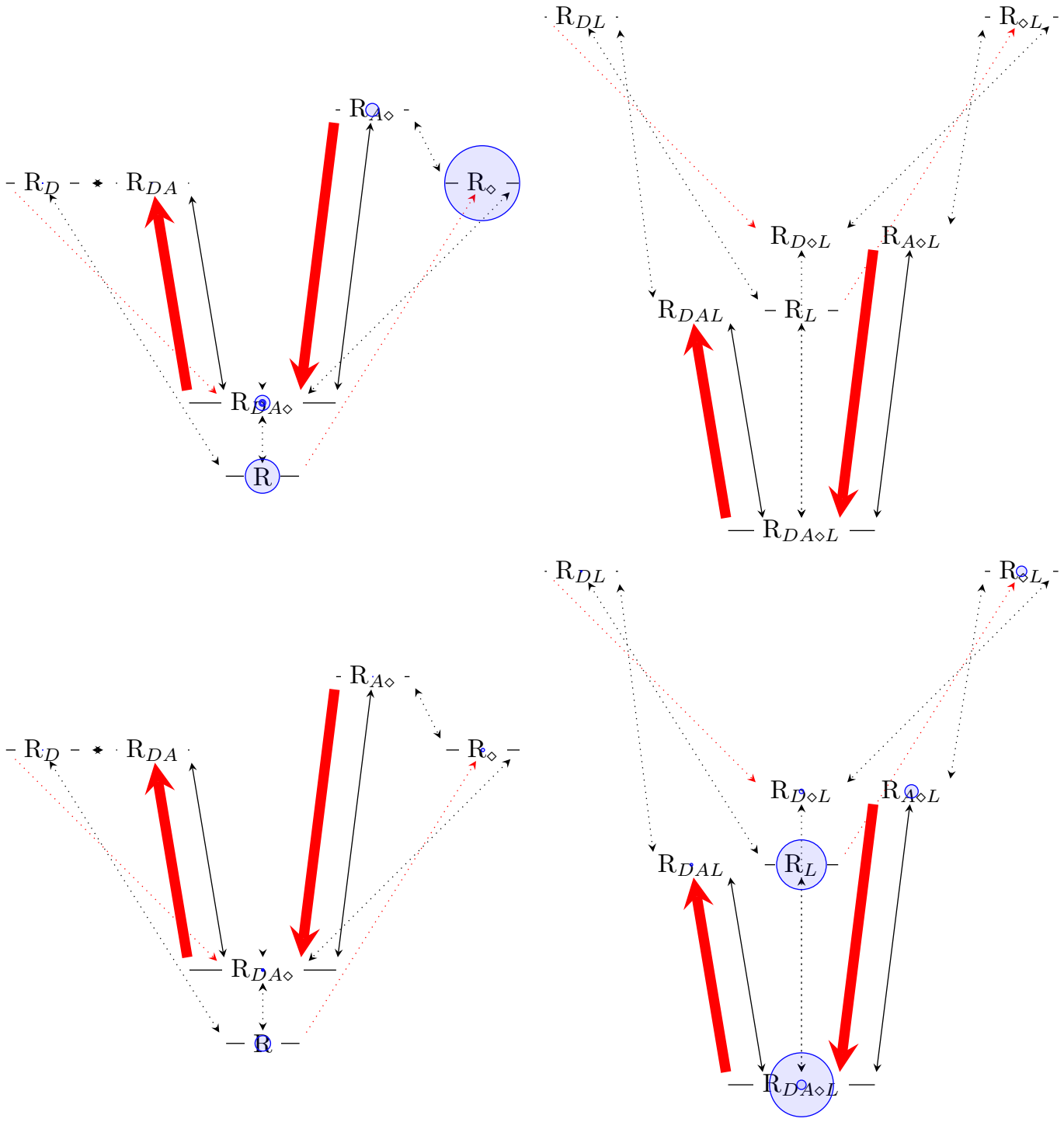

Figure 13: Receptor energy state scheme of CheD - Push hypothesis at 200 and 400 time units. $E_A^0 = 1.0$, $E_D^0 = 4.0$, $E_M^0 = 4.0$, $E_A^M = 0.0$, $E_D^M = -7.0$, $E_A^D = -1.0$, $E_A^L = -4.0$, $E_L^0 = -2.0$. $k_{AM}^{CheBp} = 1.0$, $k_{0M}^{CheBp} = 0.0$, $k_{AM}^{CheR} = 0.0$, $k_{0M}^{CheR} = 0.1$